Turbulence, Heat and Mass Transfer 8

Proceedings of the Eight International Symposium
On Turbulence, Heat and Mass Transfer
Sarajevo, Bosnia and Herzegovina, 15-18 September, 2015

Edited by

K. HANJALIĆ
Delft University of Technology, The Netherlands, and
Novosibirsk State University, Russia

T. MIYAUCHI
Tokyo Institute of Technology, and
Meiji University, Japan

D. BORELLO
Sapienza University of Rome, Italy

M. HADŽIABDIĆ
International University of Sarajevo, Bosnia and Herzegovina

P. VENTURINI
Sapienza University of Rome, Italy

Begell House Inc.
New York, Wallingford (UK)

International
Centre for Heat
and Mass Transfer

Cover illustration: *THMT from micro to macro scales*: *SGS heat flux in hydrogen-air premixed flame (from Hiraoka et al., p. 501); pollutant clouds in downtown Sarajevo during winter inversion with a mild wind (URANS, from Kenjereš et al. p. 719).*

Turbulence, Heat and Mass Transfer 8

Proceedings of the Eight International Symposium on Turbulence, Heat and Mass Transfer, Sarajevo, Bosnia and Herzegovina, September 15-18 2015/ K. Hanjalić, T. Miyauchi, D. Borello. M. Hadžiabdić, P. Venturini (Editors); Begell House Inc.

ISSN 2377-2816 (Online);	ISBN: 978-1-56700-427-4 (Online)
ISSN 2377-4169 (CD-ROM)	ISBN: 978-1-56700-428-8 (CD-ROM)

Detailed all inquiries to Begell House Inc., 50 Cross Highway, Redding, CT 06896, USA

Printed in Sarajevo, Bosnia and Herzegovina.

Turbulence, Heat and Mass Transfer 8

Large eddy simulation of MHD turbulence decay at different magnetic Reynolds number

D. B. Zhakebayev[1], A. K. Khikmetov[1], A. U. Abdibekova[1]

[1]*Departament of Mathematical and computer modelling, Kazakh National University named after al- Farabi, al-Farabi 71, 050012 Almaty, Kazakhstan, daurjaz@mail.ru*

Abstract – We consider the numerical simulation of homogeneous magnetohydrodynamic turbulence decay depending on magnetic Reynolds number based on large eddy simulation. To close magnetohydrodynamic equation system the modified dynamic model is used and calculated at each time steps. Depending on the different magnetic Reynolds number the variation of the kinetic and magnetic energies of turbulence with time, and depending on the time the micro- and macro-scale turbulence were obtained.

1. Introduction

In spite of the large number of publications in this field, the study of the homogeneous magnetohydrodynamic (MHD) turbulence decay process is a relevant task for researchers of several generations. The influence of the magnetic field on conducting fluids is studied in different scientific fields and applied in engineering and technology. Therefore, investigations of the MHD turbulence decay is an important problem for astrophysical and geophysical phenomena formation, MHD generators, plasma accelerators and engines [1-4].

The research problems of the magnetic field influence on electrically conducting fluids are split in three types:

1. Study of MHD turbulence at a constant value of the magnetic field.
2. Study the magnetic field self-excitation at a given velocity of flow.
3. Study of the magnetic field self-excitation and motion of a conducting fluid considering, at the same time, the acting forces.

This work is devoted to the study of the magnetic field self-excitation and to the motion of a conducting fluid, at the same time taking into account the acting forces. Although a lot of authors have dedicated their works to this field it is still relevant today. The results of study this problem are presented in [5] the influence of external magnetic field on the decay of MHD turbulent flow at the low magnetic Reynolds number by LES and DNS methods, and demonstrated that magnetic field in the start begins to decay when exposed to the total kinetic energy. This effect is consistent with Joule dissipation. LES method has shown excellent result in adaptation Smagorinsky dynamic model to the flow and the applied magnetic field through the dynamic procedure. A similar picture of the decay was not reported by the authors, Knaepen and Moin, because their main objective was the evaluation of the model adequacy for the LES and DNS methods.

Later, a resembling problems for anisotropy of MHD turbulence were researched by [6, 7], which reflected the change in the turbulence statistical parameters as a result of an imposed magnetic field influence. The contribution of these scientists in this area of expertise is determined by proving that the behavior of two- and three-dimensional structures varies

substantially.

In addition, investigation of pseudospectral direct numerical simulation, with up to 1024^3 nodes, three-dimensional incompressible MHD turbulence, and with no mean magnetic field in a high resolution was detailed in [8]. The study was carried out considering various statistical properties of both decreasing and statistically steady MHD turbulence on the magnetic Prandtl number Pm taken over a wide range of $0.01 \le Pm \le 10$. Turbulent characteristics were obtained at a constant magnetic viscosity for different values of kinetic viscosity.

Therefore, there is a need to examine this process over a wide range of Re_m numbers to determine the pattern of the magnetic field impact on the turbulence decay for fluids that vary in their electrical conductivity. It is known, when the Re_m number is small, the impact of the magnetic field on the kinetic energy is significant because the turbulence degeneration is faster than in the case of a large Re_m number when the impact is negligible, and the process is similar to the case of an isotropic turbulence. This effect also demonstrates the process dynamics with various Alfvén numbers. This work is devoted to the study of the magnetic field self-excitation and to the motion of a conducting fluid, at the same time taking into account the acting forces. The idea is to specify initial conditions in the phase space for a velocity and magnetic fields, which satisfy the condition of continuity. The given initial condition with the phase space is translated into physical space using a Fourier transform. The obtained velocity and magnetic fields are used as initial conditions for the filtered MHD equations. Further, the unsteady three-dimensional MHD equation is solved to simulate the homogeneous MHD turbulence decay.

2. Problem formulation

The problem is numerically modelled by solving the non-stationary filtered magnetic hydrodynamics equations in conjunction with the continuity equation in the Cartesian coordinate system in a non-dimensional form:

$$\begin{cases} \dfrac{\partial \overline{u}_i}{\partial t} + \dfrac{\partial\left(\overline{u}_i \overline{u}_j\right)}{\partial x_j} = -\dfrac{\partial \overline{p}}{\partial x_i} + \dfrac{1}{\mathrm{Re}}\left(\dfrac{\partial^2 \overline{u}_i}{\partial x_j^2}\right) - \dfrac{\partial \tau_{ij}^u}{\partial x_j} + A\dfrac{\partial}{\partial x_j}\left(\overline{H}_i \overline{H}_j\right), \\ \dfrac{\partial \overline{u}_i}{\partial x_i} = 0, \\ \dfrac{\partial \overline{H}_i}{\partial t} + \dfrac{\partial}{\partial x_j}(\overline{u}_j \overline{H}_i - \overline{H}_j \overline{u}_i) = \dfrac{1}{\mathrm{Re}_m}\dfrac{\partial^2 \overline{H}_i}{\partial x_j^2} - \dfrac{\partial \tau_{ij}^H}{\partial x_j}, \\ \dfrac{\partial \overline{H}_i}{\partial x_i} = 0, \\ \textit{where}\ \ \tau_{i,j}^H = \left(\overline{(u_i u_j)} - (\overline{u}_i \overline{u}_j)\right) - \left(\overline{(H_i H_j)} - (\overline{H}_i \overline{H}_j)\right), \\ \qquad \tau_{i,j}^u = \left(\overline{(u_i H_j)} - (\overline{u}_i \overline{H}_j)\right) - \left(\overline{(H_i u_j)} - (\overline{H}_i \overline{u}_j)\right). \end{cases} \tag{1}$$

where $\overline{u_i}$ $(i = 1, 2, 3)$ are the velocity components, $\overline{H}_1, \overline{H}_2, \overline{H}_3$ are the magnetic field strength components, $A = H^2/\left(4\pi\rho V^2\right) = \Pi/\mathrm{Re}_m^2$ is the Alfven number, H is the

characteristic value of the magnetic field strength, V is the typical velocity, $\Pi = (V_A L/\nu_m)^2$ is a dimensionless value (on which the value Π depends in the equation for $\overline{H}_i$). If $\Pi << 1$, then $\partial\overline{H}_i/\partial t = 0$. The publication [9] discusses in detail the physics of the phenomena related to the ability to disregard the summand $V_A = H/\sqrt{4\pi\rho}$ is the Alfven velocity, $\overline{p} = p + \overline{H}^2 A/2$ is the full pressure, t is the time, $\mathrm{Re} = LV/\nu$ is the Reynolds number, $\mathrm{Re}_m = LV/\nu_m$ is the magnetic Reynolds number, L is the typical length, ν is the kinematic viscosity coefficient, ν_m is the magnetic viscosity coefficient, ρ is the density of an electrically conducting incompressible fluid, and τ_{ij}^u, τ_{ij}^H are the subgrid - scale tensors responsible for small-scale structures to be modelled.

Periodic boundary conditions are selected at all boundaries of the considered area of the velocity components and magnetic field strength. The initial values for each velocity component and strength are defined in the form of a function, which depends on the wave numbers in the phase space [10].

3. Method to calculate the small-scale turbulence coefficient.

Along with the accepted calculated grid, a grid with twice the size of the cells along each axis is used. The large grid number cell is indicated as p, g, r (p, g, r are the axes numbered x_1, x_2, x_3 respectively), $p = 1,2,3,...,N_1/2$, $g = 1,2,3,...,N_2/2$, and $r = 1,2,3,...,N_3/2$. The cell with the number α along the axis x_1 includes the cells of the initial grid with numbers $n = 2p-1$ and $n = 2p$, where n varies within the range from 1 to N_1. Similar to the number g, for x_2 cells with numbers $m = 2g-1$ and $m = 2g$, $q = 2r-1$ and $q = 2r$ were determined. Therefore, one cell p,g,r of a large grid is the same as eight cells of the initial grid.

The average values u_1^2, u_2^2, u_3^2 for the total volume of the calculated area of the liquid flow are marked as $\langle u_1^2 \rangle, \langle u_2^2 \rangle, \langle u_3^2 \rangle$. These values can be calculated using smaller and larger calculation grids:

$$< u_i^2 >= \frac{1}{N_1 N_2 N_3} \cdot \sum_{n=1}^{N_1} \sum_{m=1}^{N_2} \sum_{q=1}^{N_3} \left[(\overline{u}_i)^2 + (u_i')^2 \right] \qquad (2)$$

where $(\overline{u}_i)^2 = \overline{u}_i \overline{u}_i$ and $(u_i')^2 = \overline{u_i' \cdot u_i'}$.

The subgrid-scale tensor for smaller cells is

$$\tau_{ij} = \overline{u_i' u_j'} = -2C_S \cdot \Delta_s{}^2 \cdot (2 \cdot \overline{S}_{ij}^s \cdot \overline{S}_{ij}^s)^{\frac{1}{2}} \cdot \overline{S}_{ij}^s \qquad (3)$$

where $\Delta_s = (\Delta_i \Delta_j \Delta_k)^{1/3}$ is the width grid filter of the small cell.

The deformation velocity calculated in smaller cells is $\overline{S}_{ij}^s = \frac{1}{2}\left(\frac{\partial \overline{u}_i^s}{\partial x_j} + \frac{\partial \overline{u}_j^s}{\partial x_i} \right)$,

where $n=\overline{1,N_1}$, $m=\overline{1,N_2}$, $q=\overline{1,N_3}$.

By substituting expression (3) into Eq. (2), we can obtain the average velocity value calculated in the smaller cells:

$$< u_i^2 >^s = \frac{1}{N_1 N_2 N_3} \cdot \sum_{n=1}^{N_1} \sum_{m=1}^{N_2} \sum_{q=1}^{N_3} \left[(\bar{u}_i^s)^2 - 2 \cdot C_S \cdot \Delta_s^2 \cdot (2 \cdot S_{ij}^s \cdot S_{ij}^s)^{\frac{1}{2}} S_{ij}^s \right] \tag{4}$$

The average velocity calculated in the larger cells is

$$< u_i^2 >^l = \frac{8}{N_1 N_2 N_3} \cdot \sum_{p=1}^{N_1/2} \sum_{g=1}^{N_2/2} \sum_{r=1}^{N_3/2} \left[(\bar{u}_i^l)^2 - 2 \cdot C_S \cdot \Delta_l^2 \cdot (2 \cdot S_{ij}^l \cdot S_{ij}^l)^{\frac{1}{2}} S_{ij}^l \right] \tag{5}$$

where $\Delta_l = (\Delta_i \Delta_j \Delta_k)^{1/3}$ is the width grid filter of the large cell, $\Delta_l = 2\Delta_s$.

The deformation velocity calculated in the larger cells is

$$\bar{S}_{ij}^l = \frac{1}{2} \left(\frac{\partial \bar{u}_i^l}{\partial x_j} + \frac{\partial \bar{u}_j^l}{\partial x_i} \right),$$

where $p = 1,2,3,...,N_1/2$, $g = 1,2,3,...,N_2/2$, $r = 1,2,3,...,N_3/2$.

$$\bar{u}_i^l(p,g,r) = \frac{1}{8} \begin{bmatrix} \bar{u}_i^s(2p-1, 2g-1, 2r-1) + \bar{u}_i^s(2p-1, 2g, 2r-1) + \bar{u}_i^s(2p-1, 2g, 2r) + \\ + \bar{u}_i^s(2p-1, 2g-1, 2r) + \bar{u}_i^s(2p, 2g-1, 2r-1) + \bar{u}_i^s(2p, 2g, 2r-1) + \\ + \bar{u}_i^s(2p, 2g, 2r) + \bar{u}_i^s(2p, 2g-1, 2r) \end{bmatrix};$$

We introduce the following notation:

$$F^u = \left(< u_1^2 >^s + < u_2^2 >^s + < u_3^2 >^s - < u_1^2 >^l - < u_2^2 >^l - < u_3^2 >^l \right)^2$$

From equations (4) and (5) we can conclude that

$$F^u = (Z^u - Y^u \cdot C_S)^2$$

where

$$Z^u = \frac{1}{N_1 N_2 N_3} \cdot \sum_{n=1}^{N_1} \sum_{m=1}^{N_2} \sum_{q=1}^{N_3} (\bar{u}_i^2)^s - \frac{8}{N_1 N_2 N_3} \cdot \sum_{p=1}^{N_1/2} \sum_{g=1}^{N_2/2} \sum_{r=1}^{N_3/2} (\bar{u}_i^2)^l$$

$$Y^u = \frac{1}{N_1 N_2 N_3} \cdot \sum_{n=1}^{N_1} \sum_{m=1}^{N_2} \sum_{q=1}^{N_3} (-2(\Delta_s)^2 (2 S_{ij}^s S_{ij}^s)^{\frac{1}{2}} S_{ij}^s) -$$

$$- \frac{8}{N_1 N_2 N_3} \cdot \sum_{p=1}^{N_1/2} \sum_{g=1}^{N_2/2} \sum_{r=1}^{N_3/2} (-2(\Delta_l)^2 (2 S_{ij}^l S_{ij}^l)^{\frac{1}{2}} S_{ij}^l).$$

The condition for achieving the minimum is

$$\frac{\partial F^u}{\partial C_S} = -2(Z^u - Y^u \cdot C_S) \cdot Y^u = 0.$$

Thus, $Z^u - Y^u \cdot C_S = 0$.

With a certain time step $Tstep$, the empirical coefficient of the viscosity model is calculated by the following formula $C_s = Z^u / Y^u$, with $Tstep = 10 \cdot \tau$, τ is the time step.

4. Method to calculate the small-scale magnetic field

Here the same grid is used, which was used to calculate the small-scale turbulence coefficient, which deals with a grid twice the size of the cells along each axis.

The average values of the magnetic field strength H_1^2, H_2^2, H_3^2 for the total volume of the calculated area of the liquid flow are marked as $\langle H_1^2 \rangle, \langle H_2^2 \rangle, \langle H_3^2 \rangle$. These values can be calculated using smaller and larger calculation grids:

$$< H_i^2 >= \frac{1}{N_1 N_2 N_3} \cdot \sum_{n=1}^{N_1} \sum_{m=1}^{N_2} \sum_{q=1}^{N_3} \left[(\overline{H}_i)^2 + (H_i')^2 \right] \tag{6}$$

where $(\overline{H}_i)^2 = \overline{H}_i \overline{H}_i$ and $(H_i')^2 = \overline{H_i' \cdot H_i'}$.

The magnetic subgrid-scale tensor for the smaller cells is

$$\tau_{ij}^H = \overline{H_i' H_j'} = -2 D_S \cdot \Delta_S{}^2 \cdot (2 \cdot \overline{J}_{ij}^s \cdot \overline{J}_{ij}^s)^{\frac{1}{2}} \cdot \overline{J}_{ij}^s \tag{7}$$

The magnetic rotation tensor calculated in the smaller cells is $\overline{J}_{ij}^s = \frac{1}{2}\left(\frac{\partial \overline{H}_i^s}{\partial x_j} - \frac{\partial \overline{H}_j^s}{\partial x_i} \right)$,

where $n = \overline{1, N_1}$, $m = \overline{1, N_2}$, $q = \overline{1, N_3}$.

By substituting expression (7) into Eq. (6), we can obtain the average velocity value calculated in the smaller cells:

$$< H_i^2 >^s = \frac{1}{N_1 N_2 N_3} \cdot \sum_{n=1}^{N_1} \sum_{m=1}^{N_2} \sum_{q=1}^{N_3} \left[(\overline{H}_i^s)^2 - 2 \cdot D_S \cdot \Delta_s^2 \cdot (2 \cdot J_{ij}^s \cdot J_{ij}^s)^{\frac{1}{2}} J_{ij}^s \right] \tag{8}$$

The average value of the magnetic field strength calculated in the larger cells is

$$< H_i^2 >^l = \frac{8}{N_1 N_2 N_3} \cdot \sum_{p=1}^{N_1/2} \sum_{g=1}^{N_2/2} \sum_{r=1}^{N_3/2} \left[(\overline{H}_i^l)^2 - 2 \cdot D_S \cdot \Delta_l^2 \cdot (2 \cdot J_{ij}^l \cdot J_{ij}^l)^{\frac{1}{2}} J_{ij}^l \right] \tag{9}$$

The magnetic rotation tensor calculated in the larger cells is

$$\overline{J}_{ij}^{l} = \frac{1}{2}\left(\frac{\partial \overline{H}_i^l}{\partial x_j} - \frac{\partial \overline{H}_j^l}{\partial x_i} \right),$$

where $p = 1, 2, 3, ..., N_1/2$, $g = 1, 2, 3, ..., N_2/2$, $r = 1, 2, 3, ..., N_3/2$.

$$\overline{H}_i^l(p,g,r) = \frac{1}{8}\begin{bmatrix} \overline{H}_i^{\mathrm{s}}(2p-1, 2g-1, 2r-1) + \overline{H}_i^{\mathrm{s}}(2p-1, 2g, 2r-1) + \\ + \overline{H}_i^{\mathrm{s}}(2p-1, 2g, 2r) + \overline{H}_i^{\mathrm{s}}(2p-1, 2g-1, 2r) + \\ + \overline{H}_i^{\mathrm{s}}(2p, 2g-1, 2r-1) + \overline{H}_i^{\mathrm{s}}(2p, 2g, 2r-1) + \\ + \overline{H}_i^{\mathrm{s}}(2p, 2g, 2r) + \overline{H}_i^{\mathrm{s}}(2p, 2g-1, 2r) \end{bmatrix};$$

We introduce the following notation:

$$F^H = \left(< H_1^2 >^s + < H_2^2 >^s + < H_3^2 >^s - < H_1^2 >^l - < H_2^2 >^l - < H_3^2 >^l \right)^2$$

From equations (8) and (9) it yields

$$F^H = (Z^H - Y^H \cdot D_S)^2$$

where

$$Z^H = \frac{1}{N_1 N_2 N_3} \cdot \sum_{n=1}^{N_1} \sum_{m=1}^{N_2} \sum_{q=1}^{N_3} (\overline{H}_i^2)^s - \frac{8}{N_1 N_2 N_3} \cdot \sum_{p=1}^{N_1/2} \sum_{g=1}^{N_2/2} \sum_{r=1}^{N_3/2} (\overline{H}_i^2)^l$$

$$Y^H = \frac{1}{N_1 N_2 N_3} \cdot \sum_{n=1}^{N_1} \sum_{m=1}^{N_2} \sum_{q=1}^{N_3} (-2(\Delta_s)^2 (2 J_{ij}^s J_{ij}^s)^{\frac{1}{2}} J_{ij}^s) -$$

$$- \frac{8}{N_1 N_2 N_3} \cdot \sum_{p=1}^{N_1/2} \sum_{g=1}^{N_2/2} \sum_{r=1}^{N_3/2} (-2(\Delta_l)^2 (2 J_{ij}^l J_{ij}^l)^{\frac{1}{2}} J_{ij}^l).$$

The condition for achieving the minimum is

$$\frac{\partial F^H}{\partial D_S} = -2(Z^H - Y^H \cdot D_S) \cdot Y^H = 0$$

Hence, $Z^H - Y^H \cdot D_S = 0$

Thus, the empirical coefficient of the viscosity model for the magnetic field at a certain time step *Tstep* assumes the following form: $D_s = Z^H / Y^H$.

5. Numerical method

To solve the problem of homogeneous incompressible MHD turbulence, a scheme of splitting by physical parameters is used. The following physical interpretation of the splitting diagram is suggested. At the first stage, the Navier–Stokes equation is solved with no pressure

consideration. For the approximation of convective and diffusion equation members, a compact scheme of an increased order of accuracy is used [11]. At the second stage, the Poisson equation is solved, which is derived from the continuity equation by considering the velocity fields of the first stage. For the 3D Poisson equation, an original solution algorithm has been developed: a spectral transform in combination with the matrix run. At the third stage, the obtained pressure field is used to recalculate the final velocity field. At the fourth stage, the obtained velocity field is used to solve an equation in order to obtain the components of the magnetic field strength, which are included in the initial equation.

6. Algorithm to solve the equation of magnetic field strength

Let us consider Eq. (1) as the first component of the magnetic field strength:

$$\frac{\partial H_1}{\partial t}+\frac{1}{\mathrm{Re}_m}\frac{\partial^2 H_1}{\partial x_1^2}+\frac{\partial}{\partial x_2}\left(u_2H_1-H_2u_1\right)-\frac{1}{\mathrm{Re}_m}\frac{\partial^2 H_1}{\partial x_2^2}+$$
$$+\frac{\partial}{\partial x_3}\left(u_3H_1-H_3u_1\right)-\frac{1}{\mathrm{Re}_m}\frac{\partial^2 H_1}{\partial x_3^2}=-\left(\frac{\partial \tau_{11}^H}{\partial x_1}+\frac{\partial \tau_{12}^H}{\partial x_2}+\frac{\partial \tau_{13}^H}{\partial x_3}\right). \tag{10}$$

The strength of the magnetic field is found using the fractional step method. A run method is used at each stage of the fractional step method, i.e. a step-by step definition of the magnetic field strength values.

At the first stage, the magnetic field strength $H_1^{n+\frac{1}{3}}$ is found in the direction of the coordinate x_1:

$$\frac{H_{1i,j,k}^{n+\frac{1}{3}}-H_{1i,j,k}^{n}}{\tau}=\frac{1}{2}\left[\Lambda_1 H_{1i,j,k}^{n+\frac{1}{3}}+\Lambda_1 H_{1i,j,k}^{n}\right]+\Lambda_2 H_{1i,j,k}^{n}+\Lambda_3 H_{1i,j,k}^{n}+f_{1i,j,k}^{n}. \tag{11}$$

The operator $\Lambda_1 H_1$ is

$$\Lambda_1 H_1=\frac{1}{\mathrm{Re}_m}\frac{\partial^2 H_1}{\partial x_1^2}+\frac{\partial}{\partial x_1}\left(-\tau_{11}^H\right),$$

where the viscosity model and the magnetic rotation tensor are, respectively,

$$\tau_{11}^H=-2\eta_t\cdot J_{11},$$

$$J_{11}=\frac{1}{2}\left(\frac{\partial H_1}{\partial x_1}-\frac{\partial H_1}{\partial x_1}\right)=0.$$

Similarly, the operator $\Lambda_2 H_1$ is

$$\Lambda_2 H_1 = -\frac{\partial}{\partial x_2}(u_2 H_1) + \frac{1}{\mathrm{Re}_m}\frac{\partial^2 H_1}{\partial x_2^2} + \frac{\partial}{\partial x_2}\left(-\tau_{12}^H\right),$$

$$\tau_{12}^H = -2\eta_t \cdot J_{12},$$

$$J_{12} = \frac{1}{2}\left(\frac{\partial H_1}{\partial x_2} - \frac{\partial H_2}{\partial x_1}\right).$$

For the operator $\Lambda_3 H_1$,

$$\Lambda_3 H_1 = -\frac{\partial}{\partial x_3}(u_3 H_1) + \frac{1}{\mathrm{Re}_m}\frac{\partial^2 H_1}{\partial x_3^2} + \frac{\partial}{\partial x_3}\left(-\tau_{13}^H\right),$$

$$\tau_{13}^H = -2\eta_t \cdot J_{13},$$

$$J_{13} = \frac{1}{2}\left(\frac{\partial H_1}{\partial x_3} - \frac{\partial H_3}{\partial x_1}\right),$$

$$f_1 = \frac{\partial}{\partial x_2}(H_2 u_1) + \frac{\partial}{\partial x_3}(H_3 u_1)$$

Writing the operator $\Lambda_1 H_1$ in the finite difference form,

$$\frac{\partial^2 H_1}{\partial x_1^2} = \frac{(H_1)_{i+1,j,k} - 2(H_1)_{i,j,k} - (H_1)_{i-1,j,k}}{\Delta x_1^2},$$

$$\frac{\partial}{\partial x_1}\left(-\tau_{11}^H\right) = 0, \tag{12}$$

are determined as a convective member for the operator $\Lambda_2 H_1$ on a staggered grid as

$$\frac{\partial(u_2 H_1)}{\partial x_2} = \frac{A_y \cdot \left((H_1)_{i,j+1,k} + (H_1)_{i,j,k}\right) - B_y\left((H_1)_{i,j,k} + (H_1)_{i,j-1,k}\right)}{2\Delta x_2},$$

where $A_y = (u_2)_{i,j+\frac{1}{2},k}$ and $B_y = (u_2)_{i,j-\frac{1}{2},k}$.

Similarly, the diffusion member for the operator $\Lambda_2 H_1$ is

$$\frac{\partial^2 H_1}{\partial x_2^2} = \frac{(H_1)_{i,j+1,k} - 2(H_1)_{i,j,k} + (H_1)_{i,j-1,k}}{2\Delta x_2^2}, \tag{13}$$

In addition, a strength tensor is determined for the operator $\Lambda_2 H_1$:

$$\frac{\partial}{\partial x_2}\left(-\tau_{21}^H\right)=\frac{\partial}{\partial x_2}\left(2\eta_t\cdot J_{12}\right)=$$

$$=\frac{2}{2\cdot\Delta x_2}\left[\left(\eta_t\right)_{i,j+\frac{1}{2},k}\cdot\left[\frac{\left(H_1\right)_{i,j+1,k}-\left(H_1\right)_{i,j,k}}{\Delta x_2}-\frac{\left(H_2\right)_{i+1,j,k}-\left(H_2\right)_{i,j,k}}{\Delta x_1}\right]-\right.$$

$$\left.-\left(\eta_t\right)_{i,j-\frac{1}{2},k}\cdot\left[\frac{\left(H_1\right)_{i,j,k}-\left(H_1\right)_{i,j-1,k}}{\Delta x_2}-\frac{\left(H_2\right)_{i,j,k}-\left(H_2\right)_{i-1,j,k}}{\Delta x_1}\right]\right]$$

Similarly, the operator $\Lambda_3 H_1$ is determined and, correspondingly, the convective term is

$$\frac{\partial\left(u_3H_1\right)}{\partial x_3}=\frac{A_z\cdot\left(\left(H_1\right)_{i,j,k+1}+\left(H_1\right)_{i,j,k}\right)-B_z\left(\left(H_1\right)_{i,j,k}+\left(H_1\right)_{i,j-1,k}\right)}{2\Delta x_3} \tag{14}$$

where $A_z=\left(u_3\right)_{i,j,k+\frac{1}{2}}$, $B_z=\left(u_3\right)_{i,j.k-\frac{1}{2}}$

The diffusion member for the operator $\Lambda_3 H_1$ is

$$\frac{\partial^2 H_1}{\partial x_3^2}=\frac{\left(H_1\right)_{i,j,k+1}-2\left(H_1\right)_{i,j,k}+\left(H_1\right)_{i,j,k-1}}{2\Delta x_3^2}$$

and the strength tensor is

$$\frac{\partial}{\partial x_3}\left(-\tau_{13}^H\right)=\frac{\partial}{\partial x_3}\left(2\eta_t\cdot J_{13}\right)=$$

$$=\frac{2}{2\cdot\Delta x_3}\left[\left(\eta_t\right)_{i,j,k+\frac{1}{2}}\cdot\left[\frac{\left(H_1\right)_{i,j,k+1}-\left(H_1\right)_{i,j,k}}{\Delta x_3}-\frac{\left(H_3\right)_{i+1,j,k}-\left(H_3\right)_{i,j,k}}{\Delta x_1}\right]-\right.$$

$$\left.-\left(\eta_t\right)_{i,j,k-\frac{1}{2}}\cdot\left[\frac{\left(H_1\right)_{i,j,k}-\left(H_1\right)_{i,j,k-1}}{\Delta x_3}-\frac{\left(H_3\right)_{i,j,k}-\left(H_3\right)_{i-1,j,k}}{\Delta x_1}\right]\right],$$

As a result, we have

$$\frac{\left(H_1\right)_{i,j,k}^{n+\frac{1}{3}}+\left(H_1\right)_{i,j,k}^{n}}{\tau}=\frac{1}{2}\left[\frac{1}{\mathrm{Re}_m}\frac{\left(H_1\right)_{i+1,j,k}^{n+\frac{1}{3}}-2\left(H_1\right)_{i,j,k}^{n+\frac{1}{3}}+\left(H_1\right)_{i-1,j,k}^{n+\frac{1}{3}}}{\Delta x_1^2}+\Lambda_1\left(H_1\right)_{i,j,k}^{n}\right]+ \tag{15}$$

$$+\Lambda_2\left(H_1\right)_{i,j,k}^{n}+\Lambda_3\left(H_1\right)_{i,j,k}^{n}+\left(f_1\right)_{i,j,k}.$$

The equation is solved by the run method and found to be $\left(H_1\right)_{i,j,k}^{n+\frac{1}{3}}$. The $\left(H_1\right)_{i,j,k}^{n+\frac{2}{3}}$ and $\left(H_1\right)_{i,j,k}^{n+1}$ components of the magnetic field strength are defined in a similar way. Thus, all the components of the magnetic field strength have been determined in this way.

7. Numerical modelling results

The numerical model allowed to describe the homogeneous magneto hydrodynamic turbulence decay based on large eddy simulation. For this task, the kinematic viscosity $\nu = 10^{-4}$ was taken constant and the magnetic Reynolds number was set in the range $\mathrm{Re}_m = 10^3 \div 10^4$. The characteristic values of the velocity, length, and magnetic field strength were taken equal to $U_{char} = 1, L_{char} = 1, H_{char} = 1$, respectively. The Alfven number, characterizing the motion of conductive fluid for various magnetic Reynolds numbers, was $A = Ha^2 / \mathrm{Re}_m \cdot \mathrm{Re}$, where the Hartmann number was $Ha = 1$.

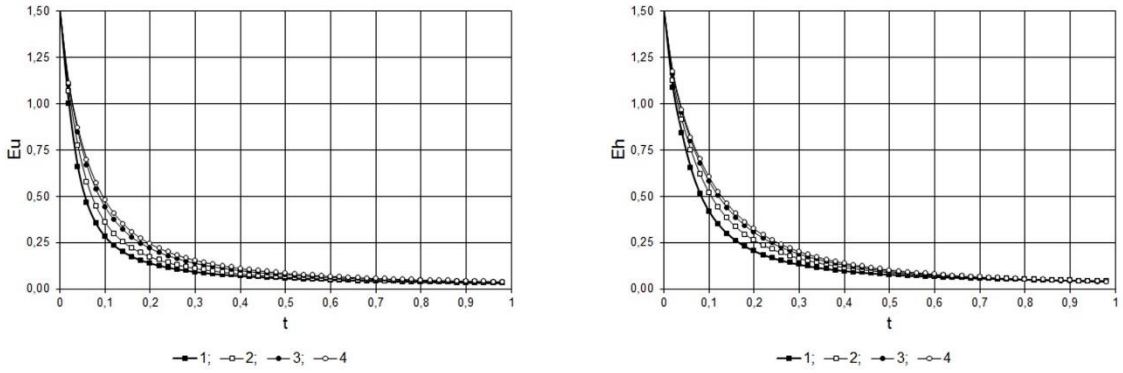

a) b)

Figure 1: Variation of a) kinetic turbulent energy b) magnetic energy vs. magnetic Reynolds numbers at different points in time: 1) $\mathrm{Re}_m = 10^3$; 2) $\mathrm{Re}_m = 2 \cdot 10^3$; 3) $\mathrm{Re}_m = 5 \cdot 10^3$; 4) $\mathrm{Re}_m = 10^4$.

For the calculations, the grid 128x128x128 was used. The time step was taken equal to $\Delta\tau = 0.001$. As a result of the simulation with different magnetic Reynolds numbers, the following turbulence characteristics were obtained: kinetic energy, magnetic energy, integral scale, Taylor scale, transverse and longitudinal correlation functions. The results displayed in Fig. 1 shows the decay of kinetic and magnetic energies calculated at different magnetic Reynolds numbers. Figs. 1 shows the dynamics of the mutual influence of magnetic and kinetic energies at different time instants: at the initial time, the kinetic and magnetic energies were given the same; at the next instant when a fluid with high conductivity was studied. The decay of MHD turbulence occurred faster than when Re_m started to rise, which specifies a fluid with smaller conductivity, and at $\mathrm{Re}_m = 10^4$ the decay of MHD turbulence practically corresponded to the decay of isotropic turbulence [12].

According to the semi-empirical theory of turbulence, the integral scale must grow with time. The results presented in Fig. 2a illustrates the effect of magnetic Reynolds number on the internal structure of MHD turbulence. A variation of the coefficient of magnetic viscosity leads to a proportional change in integral scale. Fig.2a shows that the size of large eddies rapidly increases at a small magnetic Reynolds number $\mathrm{Re}_m = 10^3$ than in the case, when $\mathrm{Re}_m = 10^4$, which leads to fast energy dissipation. Fig. 2b shows the change of the Taylor microscale at different magnetic Reynolds numbers. It can be seen in the case with $\mathrm{Re}_m = 10^3$ when the magnetic Reynolds number is large, the dissipation rate increases. In the case $\mathrm{Re}_m = 10^4$ when the magnetic Reynolds number is smaller, the scale gradually increases, and the small-scale structure of turbulence tends to slow isotropy. This also

indicates that with small Re_m numbers the decay of isotropic turbulence occurs faster than in the case when Re_m is high.

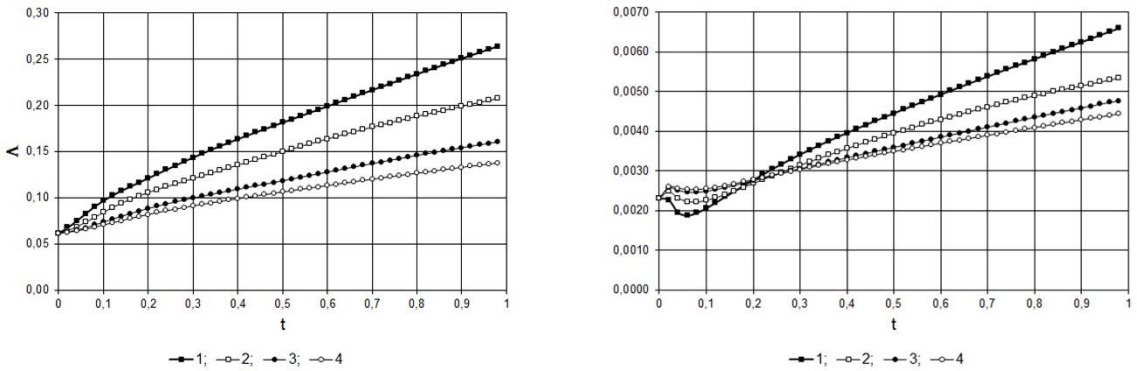

a) b)

Figure 2: Change of the a) integral turbulence scale and b) Taylor scale calculated at different magnetic Reynolds numbers at different points in time: 1) $\mathrm{Re}_m = 10^3$; 2) $\mathrm{Re}_m = 2 \cdot 10^3$; 3) $\mathrm{Re}_m = 5 \cdot 10^3$; 4) $\mathrm{Re}_m = 10^4$.

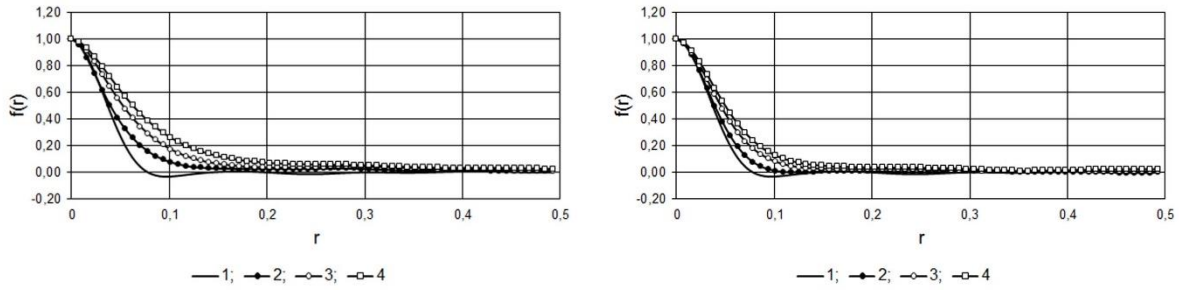

a) b)

Figure 3: Change of the longitudinal correlation function $f(r)$ when (a) $\mathrm{Re}_m = 10^3$ and (b) $\mathrm{Re}_m = 10^4$ at different points in time: 1) $t = 0.1$; 2) $t = 0.2$; 3) $t = 0.3$; 4) $t = 0.5$.

The correlation function expresses an averaged by volume correlation ratio between the velocity components at various points: the farther points are located between different components of the velocity, the smaller ones should be the correlation coefficients, i.e. they should be close to zero. Fig. 3a shows the change in longitudinal correlation function $f(r)$ in time calculated at $\mathrm{Re}_m = 10^4$ and $\mathrm{Re}_m = 10^3$. It is seen that, when being increased, the function value r tends to zero. The character of the correlation change corresponds to the change of the correlation functions given in [13].

8. Conclusions

Based on the LES method, the influence of magnetic Reynolds number on the decay of uniform magnetohydrodynamic turbulence has been numerically modelled. The obtained results allow to sufficiently accurately calculate the variations of the characteristics of uniform MHD turbulence with time at large magnetic Reynolds numbers. A numerical algorithm has been developed to solve unsteady three-dimensional magnetohydrodynamic equations as well as to model the MHD turbulence decay at different magnetic Reynolds numbers.

A numerical algorithm has been developed to solve unsteady three-dimensional magnetohydrodynamic equations as well as to model the MHD turbulence decay at different magnetic Reynolds numbers. Physical processes and phenomena of uniform MHD turbulence were identified in the numerical simulation.

References

1. G.K. Batchelor. On the spontaneous magnetic field in a conducting liquid in turbulent motion. *Proc. Roy. Soc*. A201, 16, 405–416, 1950.
2. U. Schumann. Numerical simulation of the transition from three- to two-dimensional turbulence under a uniform magnetic field. *J. Fluid Mech*., 74, pp. 31–58, 1976.
3. P. Burattini, O. Zikanov, B. Knaepen. Decay of magnetohydrodynamic turbulence at low magnetic Reynolds number. *J. Fluid Mech.,* 657, pp. 502–538, 2010.
4. B. Knaepen, S. Kassinos and D. Carati. Magnetohydrodynamic turbulence at moderate magnetic Reynolds number. *J. Fluid Mech.*, 513, no. 3, pp. 199–220, 2004.
5. B. Knaepen, P. Moin. Large-eddy simulation of conductive flows at low magnetic Reynolds number. *Physics of Fluids*, 15,pp. 297-306, 2003
6. B.Knaepen, S.Kassinos and D.Carati. Magnetohydrodynamic turbulence at moderate magnetic Reynolds number. *J. Fluid Mech.*, vol. 513 (2004), no. 3, pp. 199–220.
7. O. Vorobev, A. Zikanov. Davidson and B. Knaepen. Anisotropy of magnetohydrodynamic turbulence at low magnetic Reynolds number. *J. Physics of fluids*, 17, pp. 4-11, 2005.
8. G.Sahoo, P.Perlekar, R.Panditn. Systematics of the magnetic Prandtl-number dependence of homogeneous, isotropic magnetohydrodynamic turbulence. *New J. Phys.*, 13, pp. 1367–2630, 2011.
9. V.M. Ievlev. The Method of Fractional Steps for Solution of Problems of Mathematical Physics. *Nauka*, 1975.
10. B. T. Zhumagulov, D. B. Zhakebayev, and A. U. Abdibekova. The decay of MHD turbulence depending on the conductive properties of the environment. *Magnetohydrodynamics*, 50, No. 2, 2014.
11. U.S. Abdibekov, B. T. Zhumagulov, D. B. Zhakebayev, K. Zh. Zhubat. Simulation of isotropic turbulence degeneration based on the large-eddy method. *Mathematical Models and Computer Simulations*, 5, No. 4, pp. 360-370, 2013.
12. U.S. Abdibekov, D. B. Zhakebayev. Modelling of the decay of isotropic turbulence by LES. *Journal of Physics:* Conference Series, Proceedings of the 13th European turbulence conference, Warsaw, 318, pp.327-338, 2011.
13. N. de Divitiis, Lyapunov analysis for fully developed homogeneous isotropic turbulence. *Theor. Comput. Fluid Dyn*. 25, No. 6, pp. 421–445, 2011.

Turbulence, Heat and Mass Transfer 8

Numerical modelling of convective diffusion in three-component gas mixtures

D.B. Zhakebayev [1], A.P. Kizbayev [1] , V.N. Kosov[2] and M. O.V. Fedorenko [2]

[1]*Department of Mathematical and Computer modeling, Kazakh National University named after al-Farabi, al-Farabi 71, 050038, Almaty, Kazakhstan, dauren.zhakebaev@kaznu.kz*

[2]*Institute of Experimental and Theoretical Physics, Kazakh National University named after al-Farabi, al-Farabi 71, 050038, Almaty, Kazakhstan, fedor23.04@mail.ru*

Abstract – This paper considers the numerical modeling of convective diffusion in three-component gas mixtures. The experimental results on the study of unstable diffusion process at different pressures is carried out based on the numerical solution of unsteady filtered Navier-Stokes equation, the continuity equation and equation for the concentration. Comparison of the results of numerical simulations with experimental data for the system 0.4688 He + 0.5312 Ar - N2 showed that the intensity of convective mass transfer increases at a certain critical value of pressure.

1. Introduction

The analysis of the occurrence of instability in isothermal mutual diffusion showed that the description is completely analogous to the conventional thermal convection, when the system has only one constant thermodynamic force causing convection (diffusion performs role of the thermal conductivity). In the case of the existence of two forces ∇C and ∇T at the same time we will get qualitatively new effects [1], that the convective unstable states are possible in negative direction of the density gradient (at the bottom of the mixture more dense). Thus, the emergence of concentration convection in the gas mixture contained in the gravity field is possible in the case of inhomogeneous distribution of composition (density) in the channel of a diffusion cell. Based on experimental studies the occurrence of diffusion instability in three-component gas mixtures subject to a number of necessary conditions is shown in [2]:

1) Binary gas mixture (1 + 2) is located at the top, pure gas (3) - at the bottom, $\rho_2 > \rho_3 > \rho_1$; $\rho_{(1+2)} < \rho_3$; $D_{13} > D_{23}$;

2) Binary gas mixture (1+2) is located at the bottom, pure gas (3) – at the top, $\rho_2 > \rho_3 > \rho_1$; $\rho_{(1+2)} > \rho_3$; $D_{13} > D_{23}$;

3) Binary gas mixture (1 + 2) is located at the top, binary gas mixture (3+2) – at the bottom, $\rho_2 > \rho_3 > \rho_1$; $\rho_{(3+2)} > \rho_{(1+2)}$; $D_{12} > D_{32}$;

4) Binary gas mixture (1+2) and pure gas (3) may be disposed either above or below, $\rho_2 > \rho_3 > \rho_1$; $\rho_{(1+2)} = \rho_3$; $D_{13} > D_{23}$; in this version the unstable process is possible at any orientation mixtures, but only for different parameters, particularly pressure.

Necessary conditions for the onset of convection in the case of diffusive mixing should be complemented by the following sufficient conditions:

1) The gas mixture must consist of components that have diffusion coefficients, which differ several times (e.g., D_{He-Ar} is bigger over about three times than D_{Ar-N_2});

2) The instability occurs at certain concentration ranges of components;

3) The pressure effect is significant;

4) A diameter of the diffusion channel should not be less than a certain size;

5) The temperature influences on the occurrence of instability;

6) In some three - component gas mixtures the instability occurs independently from the initial orientation of the components in the diffusion apparatus;

7) The occurrence of the unstable process is more possible with decreasing diffusing mixture viscosity.

The effects caused by the presence of two thermodynamic forces can significantly become complicated by the presence of cross-effects. In this case, we have two reasons for occurrence of thermal convection concentration: heterogeneity of both the temperature and the concentration. A phenomenon, which leads to the loss of stability in such systems, has been called "double-diffusive convection" [3].

Since the isothermal diffusion in the triple mixtures is also characterized by the presence of two independent partial concentration gradients, then it seems urgent to analysis of the most characteristic moments arising in the study of phenomena the convection of class "double-diffusive" or convective diffusion.

The physical meaning of the paradox of instability (convective diffusion) in the three-component gas mixtures can be represented in the following way. The element of medium, which shifted randomly upward, goes into the mixture with a lower density, according to another composition. Due to differences in the coefficients of mutual diffusion of components the transverse diffusion in the first instance tends to equalize the concentration of the light component, its insufficiency is quickly compensated, and the element, which has been displaced, becomes lighter of environment, continues float up, creating instability. A similar situation for non-isothermal case in a binary liquid mixture has been described by several authors [1, 3, 4].

Predict the region of thermodynamic parameters of mechanical equilibrium instability with diffusion can be within the stability theory [4 - 7]. It should be noted that in the study of non-stationary processes, this approach may not accurately determine the critical conditions of "diffusion-convection" transition process. Studying the dynamics of convective flows and evaluation of multicomponent mass transfer kinetics in the developed instability is not possible within the framework of the instability theory. Such problem can be solved by numerical methods of mathematical modelling. The intermediate velocity field is obtained by using fractional step method in combination with TDMA algorithm. At the second step the Poisson equation for pressure is solved using the obtained intermediate velocity field. At the third step is assumed that the transfer of mass is carried out only by the pressure gradient. At each stage of the fractional step method is used the TDMA algorithm to find landmark values of the intermediate values of the velocity field. At the last stage of splitting scheme, the finite field of velocity adjusted for pressure is obtained [8 - 10].

This scheme was approved for the system $0.4722\,He + 0.5278\,Ar - N_2$. For this system the velocity profiles were obtained at different concentrations and experiences values of pressure that remain flat at the pressure below the critical value, at which the transition occurs "diffusion - convection", but at the critical pressure and concentrations velocity profiles of the components the front is not flat , which indicates the presence of upstream and downstream flow.

The purpose of this paper is to simulate numerically the formation mechanism of convective flows in the diffusion of three-component gas mixtures.

2. Numerical model

Numerical simulation of the problem is based on the solution of unsteady Navier-Stokes equation with the continuity and concentration equations (1):

$$\begin{cases} \dfrac{\partial \vec{u}_i}{\partial t} = -\nabla p + \nabla^2 \vec{u} + (R_1 c_1 \tau_{11} + R_2 c_2)\vec{\gamma}, \\ \dfrac{\partial c_1}{\partial t} + \vec{v}\nabla c_1 = \dfrac{1}{\mathrm{Pr}_{11}} \nabla^2 c_1 + \dfrac{A_2}{A_1} \dfrac{1}{\mathrm{Pr}_{12}} \nabla^2 c_2, \\ \dfrac{\partial c_2}{\partial t} + \vec{v}\nabla c_2 = \dfrac{A_1}{A_2} \dfrac{1}{\mathrm{Pr}_{21}} \nabla^2 c_1 + \dfrac{1}{\mathrm{Pr}_{22}} \nabla^2 c_2, \\ div\ \vec{v} = 0. \end{cases} \tag{1}$$

where D_{ij}^* - practical diffusion coefficient, $\mathrm{Pr}_{ii} = \nu / D_{ii}^*$ - diffusion Prandtl number, $R_i = g\beta_i A_i d^4 / \nu D_{ii}^*$ - partial Rayleigh number, $\tau_{ij} = D_{ij}^* / D_{22}^*$ - parameter of the relationship between practical diffusion coefficients.

Boundary conditions consist of the following boundary conditions (2):

$$\vec{u} = 0,\ \frac{\partial c_i}{\partial n} = 0, \tag{2}$$

where n - normal to the boundary.

3. Numerical algorithm

Splitting scheme by physical parameters is used for the numerical solution of the gas motion in the cylindrical region. It is proposed the following physical interpretation of the given splitting scheme.

$$1.\quad \frac{\bar{u}^* - \bar{u}^n}{\tau} = -\bar{u}^n \nabla \bar{u}^* + \Delta \bar{u}^* + \tau_{11} Ra_1 C_1 + Ra_2 C_2,$$

$$2.\quad \Delta p = \frac{\nabla \bar{u}^*}{\tau},$$

$$3.\quad \frac{\bar{u}^{n+1} - \bar{u}^*}{\tau} = -\nabla p \tag{3}$$

$$4.\quad \frac{\bar{C}_1^{n+1} - \bar{C}_1^n}{\tau} = -\left(\bar{u}^{n+1}\nabla\right)\bar{C}_1^* + \frac{1}{\mathrm{Pr}_{11}}\Delta \bar{C}_1^* + \frac{1}{\mathrm{Pr}_{12}}\Delta \bar{C}_2^*$$

$$5.\quad \frac{\bar{C}_2^{n+1} - \bar{C}_2^n}{\tau} = -\left(\bar{u}^{n+1}\nabla\right)\bar{C}_2^* + \frac{1}{\mathrm{Pr}_{21}}\Delta \bar{C}_1^* + \frac{1}{\mathrm{Pr}_{22}}\Delta \bar{C}_2^*$$

At the first stage of the numerical splitting scheme, the transfer of momentum carried out only by convection and diffusion. Compact scheme of high order accuracy is used to approximate the convective and diffusive terms of the equation. The intermediate velocity field is calculated by the method of fractional steps, using the sweep method.

At the second stage, the pressure is calculated by using already founded intermediate velocity field.

At the third step, we assume that the transfer is carried out only by the pressure gradient. At the final step, the concentration is calculated by using finite velocity fields.

3.1 Calculation of the intermediate velocity field

The intermediate velocity field calculated by using the method of fractional steps. Sweep method for finding values of the intermediate velocity field used at the each step of the method of fractional steps.

Consider the method of fractional steps for the horizontal component of the velocity u_1 in the grid point $(i+1/2, j)$.

$$\frac{\partial \overline{u_1}}{\partial \tau}+\overline{u}_1\frac{\partial \overline{u_1}}{\partial x_1}+\overline{u}_2\frac{\partial \overline{u_1}}{\partial x_2}=\frac{\partial^2 \overline{u_1}}{\partial x_1^2}+\frac{\partial^2 \overline{u_1}}{\partial x_2^2} \tag{4}$$

At the first stage velocity u_1 is looked for in the direction of coordinates x_1:

$$\frac{\overline{u}_{1\,i+\frac{1}{2},j}^{\,n+\frac{1}{2}}-\overline{u}_{1\,i+\frac{1}{2},j}^{\,n}}{\tau}=\frac{1}{2}\left[\Lambda_1\overline{u}_{1\,i+\frac{1}{2},j}^{\,n+\frac{1}{2}}+\Lambda_2\overline{u}_{1\,i+\frac{1}{2},j}^{\,n}\right] \tag{5}$$

where

$$\Lambda_1\overline{u}_{1i+\frac{1}{2},j}=-u_1\frac{\partial \overline{u_1}}{\partial x_1}\bigg|_{i+\frac{1}{2},j}+\frac{\partial}{\partial x_1}\left(\frac{\partial \overline{u_1}}{\partial x_1}\right)\bigg|_{i+\frac{1}{2},j},$$

$$\Lambda_2\overline{u}_{1i+\frac{1}{2},j}=-u_2\frac{\partial \overline{u_1}}{\partial x_2}\bigg|_{i+\frac{1}{2},j}+\frac{\partial}{\partial x_2}\left(\frac{\partial \overline{u_1}}{\partial x_2}\right)\bigg|_{i+\frac{1}{2},j}.$$

This equation is solved by the sweep method and for result we get $\overline{u}_{1\,i+\frac{1}{2},j}^{\,n+\frac{1}{2}}$.

$$a_i\overline{u}_{1i+1,j}^{\,n+\frac{1}{2}}-b_i\overline{u}_{1i,j}^{\,n+\frac{1}{2}}+c_i\overline{u}_{1i-1,j}^{\,n+\frac{1}{2}}=-d_i, \tag{6}$$

where

$$a_i = \frac{1}{2}\left[-\bar{u}_{1i,j}^{\,n}\frac{1}{2\Delta x_1}+\frac{1}{\Delta x_1^2}\right],$$

$$b_i = \frac{1}{\tau}+\frac{1}{\Delta x_1^2},$$

$$c_i = \frac{1}{2}\left[\bar{u}_{1i,j}^{\,n}\frac{1}{2\Delta x_1}+\frac{1}{\Delta x_1^2}\right],$$

$$d_i = \frac{\bar{u}_{1i,j}^{\,n}}{\tau}+\frac{1}{2}\Lambda_2\bar{u}_{1\,i+\frac{1}{2},j}^{\,n}.$$

At the second stage velocity u_1 is looked for in the direction of coordinates x_2:

$$\frac{\bar{u}_{1\,i+\frac{1}{2},j}^{\,n+1}-\bar{u}_{1\,i+\frac{1}{2},j}^{\,n+\frac{1}{2}}}{\tau}=\frac{1}{2}\left[\Lambda_1\bar{u}_{1\,i+\frac{1}{2},j}^{\,n+\frac{1}{2}}+\Lambda_2\bar{u}_{1\,i+\frac{1}{2},j}^{\,n+1}\right]. \tag{7}$$

This equation is solved by the sweep method and for result we get $\bar{u}_{1\,i+\frac{1}{2},j}^{\,n+1}$.

$$a_j\bar{u}_{1i,j+1}^{\,n+1}-b_j\bar{u}_{1i,j}^{\,n+1}+c_j\bar{u}_{1i,j-1}^{\,n+1}=-d_j. \tag{8}$$

where

$$a_j = \frac{1}{2}\left[-\bar{u}_{2i,j}^{\,n}\frac{1}{2\Delta x_2}+\frac{1}{\Delta x_2^2}\right],$$

$$b_j = \frac{1}{\tau}+\frac{1}{\Delta x_2^2},$$

$$c_j = \frac{1}{2}\left[\bar{u}_{2i,j}^{\,n}\frac{1}{2\Delta x_2}+\frac{1}{\Delta x_2^2}\right],$$

$$d_j = \frac{\bar{u}_{1i,j}^{\,n+\frac{1}{2}}}{\tau}+\frac{1}{2}\Lambda_1\bar{u}_{1\,i+\frac{1}{2},j}^{\,n+\frac{1}{2}}.$$

Further, the vertical velocity components u_2 at the point $(i, j+1/2)$ of the grid are obtained in the similar manner. At the second stage, the poisson's equation, obtained from the continuity equation in view of the velocity field of the first stage. At the third stage, the resulting pressure field is used to recalculate the final velocity field. At the final stage, the obtained velocity field is used for solving the component concentrations equations.

3.2 Calculation of the concentration

Consider the method of fractional steps for the concentration $\overline{C_1}$ in the grid point $(i+1/2, j)$.

$$\frac{\partial \overline{C_1}}{\partial \tau}+\bar{u}_1\frac{\partial \overline{C_1}}{\partial x_1}+\bar{u}_2\frac{\partial \overline{C_1}}{\partial x_2}=\frac{1}{\mathrm{Pr}_{11}}\left(\frac{\partial^2 \overline{C_1}}{\partial x_1^2}+\frac{\partial^2 \overline{C_1}}{\partial x_2^2}\right)+\frac{1}{\mathrm{Pr}_{12}}\left(\frac{\partial^2 \overline{C_2}}{\partial x_1^2}+\frac{\partial^2 \overline{C_2}}{\partial x_2^2}\right). \tag{9}$$

In the first stage concentration is looked for in the direction of coordinates x_1:

$$\frac{\overline{C}_{1\,i+\frac{1}{2},j}^{\,n+\frac{1}{2}}-\overline{C}_{1\,i+\frac{1}{2},j}^{\,n}}{\tau}=\frac{1}{2}\left[\Lambda_1\overline{C}_{1\,i+\frac{1}{2},j}^{\,n+\frac{1}{2}}+\Lambda_2\overline{C}_{1\,i+\frac{1}{2},j}^{\,n}\right]. \tag{10}$$

where

$$\Lambda_1\overline{C}_{1\,i+\frac{1}{2},j}=-\bar{u}_1\frac{\partial \overline{C_1}}{\partial x_1}\bigg|_{i+\frac{1}{2},j}+\frac{1}{\mathrm{Pr}_{11}}\frac{\partial}{\partial x_1}\left(\frac{\partial \overline{C_1}}{\partial x_1}\right)\bigg|_{i+\frac{1}{2},j},$$

$$\Lambda_2\overline{C}_{1\,i+\frac{1}{2},j}=-u_2\frac{\partial \overline{C_1}}{\partial x_2}\bigg|_{i+\frac{1}{2},j}+\frac{1}{\mathrm{Pr}_{11}}\frac{\partial}{\partial x_2}\left(\frac{\partial \overline{C_1}}{\partial x_2}\right)\bigg|_{i+\frac{1}{2},j}$$

This equation is solved by the sweep method and for result we get $\overline{C}_{1\,i+\frac{1}{2},j}^{\,n+\frac{1}{2}}$.

$$a_i\overline{C}_{1\,i+1,j}^{\,n+\frac{1}{2}}-b_i\overline{C}_{1\,i,j}^{\,n+\frac{1}{2}}+c_i\overline{C}_{1\,i-1,j}^{\,n+\frac{1}{2}}=-d_i. \tag{11}$$

where

$$a_i=\frac{1}{2}\left[-\bar{u}_{1i,j}^{\,n}\frac{1}{2\Delta x_1}+\frac{1}{\mathrm{Pr}_{11}}\frac{1}{\Delta x_1^2}\right],$$

$$b_i=\frac{1}{\tau}+\frac{1}{\mathrm{Pr}_{11}}\frac{1}{\Delta x_1^2},$$

$$c_i=\frac{1}{2}\left[\bar{u}_{1i,j}^{\,n}\frac{1}{2\Delta x_1}+\frac{1}{\mathrm{Pr}_{11}}\frac{1}{\Delta x_1^2}\right],$$

$$d_i=\frac{\overline{C}_{1\,i,j}^{\,n}}{\tau}+\frac{1}{2}\Lambda_2\overline{C}_{1\,i+\frac{1}{2},j}^{\,n}$$

In the second stage concentration is looked for in the direction of coordinates x_2:

$$\frac{\overline{C}_{1\,i+\frac{1}{2},j}^{\,n+1} - \overline{C}_{1\,i+\frac{1}{2},j}^{\,n+\frac{1}{2}}}{\tau} = \frac{1}{2}\left[\Lambda_1 \overline{C}_{1\,i+\frac{1}{2},j}^{\,n+\frac{1}{2}} + \Lambda_2 \overline{C}_{1\,i+\frac{1}{2},j}^{\,n+1}\right]. \tag{12}$$

This equation is solved by the sweep method and for result we get $\overline{C}_{1\,i+\frac{1}{2},j}^{\,n+1}$.

$$a_j \overline{C}_{1\,i,j+1}^{\,n+1} - b_j \overline{C}_{1\,i,j}^{\,n+1} + c_j \overline{C}_{1\,i,j-1}^{\,n+1} = -d_j\,. \tag{13}$$

where

$$a_j = \frac{1}{2}\left[-\bar{u}_{2i,j}^{\,n}\frac{1}{2\Delta x_2} + \frac{1}{\mathrm{Pr}_{11}}\frac{1}{\Delta x_2^2}\right],$$

$$b_j = \frac{1}{\tau} + \frac{1}{\mathrm{Pr}_{11}}\frac{1}{\Delta x_2^2},$$

$$c_j = \frac{1}{2}\left[\bar{u}_{2i,j}^{\,n}\frac{1}{2\Delta x_2} + \frac{1}{\mathrm{Pr}_{11}}\frac{1}{\Delta x_2^2}\right],$$

$$d_j = \frac{\overline{C}_{1\,i,j}^{\,n+\frac{1}{2}}}{\tau} + \frac{1}{2}\Lambda_1 \overline{C}_{1\,i+\frac{1}{2},j}^{\,n+\frac{1}{2}} + \frac{1}{\mathrm{Pr}_{12}}\Delta\overline{C_2}..$$

Further, the concentration $\bar{C}_2$ at the grid point $(i+1/2, j)$ is obtained in similar method of fractional steps.

4. Experimental results

The pressure is an important characteristic of mass transfer in multicomponent systems. The increase in pressure can lead to a breach of sustainable diffusion process and the onset of convection. The authors of "Instabilities in ternary diffusion" Miller L., Spurling T.H., Mason E.A. [8] are one of the firsts, who drew the attention to the effect of pressure to instability, and it is studied in more detail in [9-11].

The experimental system 0.4688 He + 0.5312 Ar - N_2 is chosen to study the effect of pressure. Fig. 1 presents data for the system to the stable and unstable transfer at T = 298.0 K and different values of pressure [10].

As it is seen from the data shown in Fig. 1, at pressure fields up to 1.5 MPa the steady diffusive transport is observed, since the dimensionless criterion α = 1. The dimensionless criterion α for component *i* is determined from the ratio of the measured concentration to its theoretical value calculated under the assumption diffusion Stefan-Maxwell equations. With increasing pressure the unstable process is observed, characterized by a sharp increase in the parameter α, which indicates the occurrence of convection.

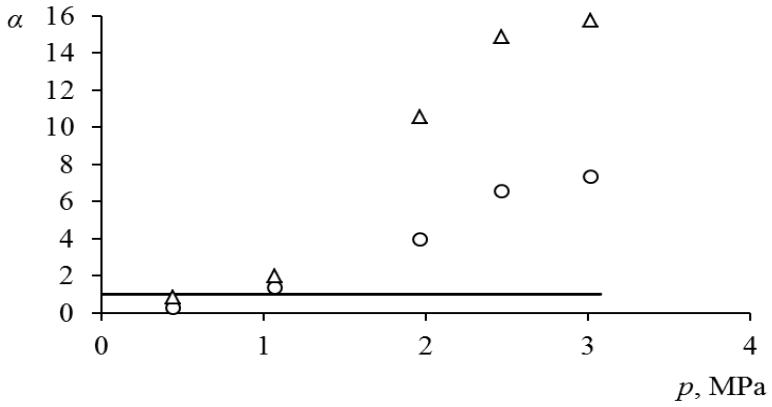

Solid line - calculation under the assumption of stable diffusion; ○ - helium; Δ - nitrogen.
Figure 1: The dependence of the parameter α on the pressure

5. Numerical results

The numerical model allows to describe the occurrence of diffusion instability depending on the pressure. For this problem the pressure is selected in the range $P \approx 0.2 \div 3.0\,MPa$. The calculations used the mesh size 128x128x128. The time step is taken as $\Delta\tau = 0.001$.

In the calculations the diffusion instability is registered at *P = 1.5 MPa*. In figure 2 the "diffusion - convection gravity concentration" transition illustrate at the moment t = 2. As can be seen from the figure 3, the oscillation amplitude of the convection is increased, indicating a violation of the diffusive instability. The vertical velocity and concentration distributions at the mid-height (y=0.5) are presented in Figure 4 and show the occurrence of diffusion instability.

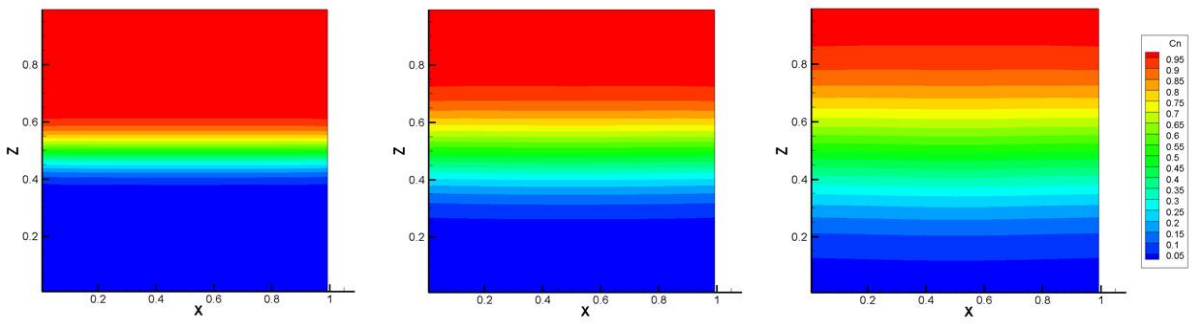

a) b) c)

Figure 2: Change of concentration of 0.5312 Ar + 0.4688 $He - N_2$ gas system at P = 1.5 MPa: $a)\ t = 0.25;\ b)\ t = 1;\ c)\ t = 2.$

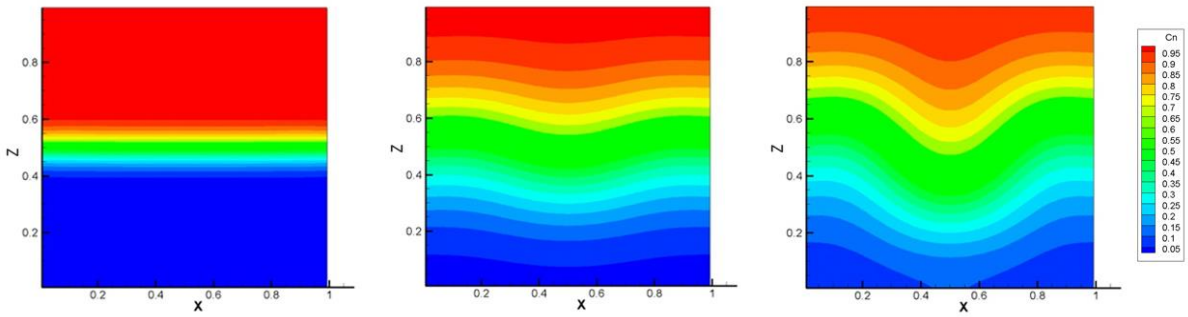

a) b) c)

Figure 3: Change of concentration of 0.5312 Ar + 0.4688 $He - N_2$ gas system at P = 2.0 MPa: $a)\ t = 0.25; b)\ t = 1; c)\ t = 2.$

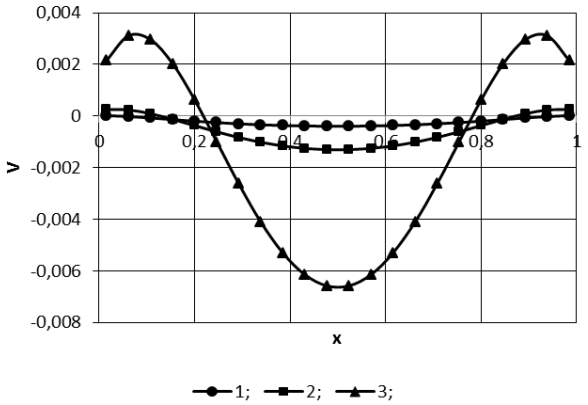

Figure 4: The velocity profile $V(x)$ in a section $y = 0.5$ at $t = 2$: 1) $P = 0.5\ MPa$; 2) $P = 1.5\ MPa$; 3) $P = 2.0\ MPa$.

7. Conclusion

This studies show, that the pressure is one of the factors contributing to the emergence of unstable diffusion process in the gas system. The critical Rayleigh number is determined basing on the numerical solution of the gas motion in the cylindrical region and solving the unsteady Navier-Stokes equation and the continuity equation with the concentration equation, which determines the transition border from the steady diffusion to the region of the concentrating gravitational convection, and shows the change of velocity profiles and component concentrations. At the critical values of pressure the velocity profiles have not flat front, which indicates the presence of upstream and downstream. Investigation of the influence pressure on the occurrence of convective diffusion has shown, that increase in pressure leads to an increase in the intensity of convective flows, i.e., to process intensification.

Comparative analysis of numerical simulation based on the method of splitting into physical parameters with the experimental data for the system 0.4688 He + 0.5312 Ar – N_2 showed qualitative and quantitative agreement. Therefore, the approach described in this investigation can be used to determine the critical parameters under which a transition from stable to unstable diffusion process is observed, characterized by the occurrence of convective flows.

References

1. D. Joseph. Stability of fluids motions. *New York, Wiley*, 1981
2. Yu. I. Zhavrin, M. S. Moldabekova, I.V. Poyarkov, V. Mukamedenkyzy. Experimental study of diffusion instability in three-component gas mixture without density gradient. *Technical Physics Letters*, 37, no. 8. pp. 721-723, 2011
3. S. Rosenblat. Thermal convection in vertical circular cylinder. *J. Fluid Mech.*, 122, pp. 395-410, 1982
4. G.Z. Gershuni and E. M. Zhukhovitskii. Convective Stability of Incompressible Fluids. *Keter, Jerusalem*, 1976
5. V. N. Kossov, D. U. Kulzhanov, I. V. Poyarkov, O.V. Fedorenko. Study of diffusion instability in some ternary gas mixtures at various temperatures. *Mod. Mech. Eng*., 3, no. 2, pp. 85-89, 2013
6. V. N. Kosov, O. V. Fedorenko, Yu. I. Zhavrin, V. Mukamedenkyzy. Instability of Mechanical Equilibrium during Diffusion in a Three-Component Gas Mixture in a vertical Cylinder with a Circular Cross Section. *Technical Physics*, 59, no. 4,pp. 482-486, 2014
7. M. K. Asembaeva, V. Mukamedenkyzy, A. T. Nysanbaeva, I. V. Poyarkov, O.V.Fedorenko. Determining the Molecular Mass Transfer Boundary in a Plane Vertical Channel with Mass Transfer. *Fluid Dynamics*,49, no. 3, pp. 403-406, 2014
8. L. Miller, T.H. Spurling, and E.A. Mason. Instabilities in ternary diffusion. *Phys. Fluids.*10, no. 8, pp. 1806-1811, 1967
9. Yu.I. Zhavrin, N.D. Kosov, S.M. Belov and S.B. Tarasov, Effect of pressure on the diffusion stability in some three-component gas mixtures. *Zh. Tekh. Fiz*., 54, no. 5, pp. 943-947, 1984
10. N. D. Kosov, Yu. I. Zhavrin, V. N. Kosov. Diffusive instability during ternary isothermal diffusion in the absence of gravitation. (*Review proceedings of Hydromech. and heat/mass transfer in microgravity), Amsterdam: Gordon and Breach Science Publishers,* pp. 531-536, 1992.
11. Yu.I. Zhavrin, V.N. Kosov, D.U. Kulzhanov and K.K. Karataeva, Effect of the pressure on the type of mixing in a three-component gas mixture containing a component possessing the properties of a real gas. *Technical Physics Letters*, 26, no. 12, pp. 1108-1109, 2000
12. U. Abdibekov; D. Zhakebaev, B. Zhumagulov. Simulation of turbulent mixing of a homogeneous liquid in the presence of an external source force. *Turbulence Heat And Mass Transfer 6*, pp. 629-632, 2009
13. D. B. Zhakebaev, U. S. Abdibekov, B. T. Zhumagulov. Numerical modeling of non-homogeneous turbulence on cluster computing system. *Notes on Numerical Fluid Mechanics (NNFM)*, 115, pp.327-338, 2011
14. D. B. Zhakebaev, B. T. Zhumagulov, A. U. Abdibekova. The decay of MHD turbulence depending on the conductive properties of the environment. *Magnetohydrodynamics*, 50, no. 2, pp. 121-138, 2014

Organizing Committee

K. Hanjalić, Chairman
T. Miyauchi, Co-Chairman
D. Borello, Symposium Secretary
M. Hadžiabdić, Organizing Secretary
J.-P. Bonnet, *University of Poitiers, France*
E. Džaferović, *University of Sarajevo, BH*
E. Ganić, *Sarajevo School of Sci. Techn. BH*
T.B. Gatski, *Old Dominion University, USA*
S.S. Girimaji, *Texas A&M University, USA*
S. Jakirlić, *Darmstadt Univ. Techn., Germany*
S. Kenjereš, *Delft Univ. of Technology, Nl*
B.E. Launder, *University of Manchester, UK*
D. Laurence, *Electricité de France*
D. Markovich, *ITP SB RAS/NSU, Russia*
I. Marusic, *University of Melbourne, Australia*
Y. Nagano , *Nagoya Inst. of Technology, Japan*
A. Pollard, *Queen's University, Canada*
F. Rispoli, *'Sapienza' University, Rome, Italy*
M. Tanahashi, *Tokyo Inst. of Techn., Japan*

Scientific Advisory Committee

R. Amano, *USA*
H.I. Andersson, *Norway*
V. Armenio, *Italy*
B. Basara, *Austria*
S. Benhamadouche, *France*
D. Bergstrom, *Canada*
B.J. Boersma, *Nl*
C.M. Casciola, *Italy*
I. Castro, *UK*
H. Choi, *Korea*
A. Corsini, *Italy*
D. Čokljat, *UK*
T.J. Craft, *UK*
L. Davidson, *Sweden*
C. Dopazo, *Spain*
S. Drobniak, *Poland*
S.E. Elghobashi, *USA*
M. Fairweather, *UK*
S. Frolov, *Russia*
S. Fu, *China*
Y. Hagiwara, *Japan*
H. Hattori, *Japan*
E. Hawkes, *Australia*
G. Hetsroni† , *Israel*
R.J.A. Howard, *France*
J. Janicka, *Germany*
T. Kajishima, *Japan*
J. Klewicki, *Australia/USA*
S. Komori, *Japan*
S. Lardeau, *UK*
R. Manceau, *France*
E. Mastorakos, UK
S. Obi, *Japan*
S-H Peng, *Sweden*
J.C. Pereira, *Portugal*
M. Reeks, *UK*
M. Van Reeuwijk, *UK*
D.J.E.M. Roekaerts, *Nl*
G.P. Romano, *Italy*
E. Serre, *France*
J. Sesterhenn, *Germany*
D.Ph. Sikovsky, *Russia*
A.P. Silva Freire, *Brazil*
A. Soldati, *Italy*
M. Strelets, *Russi*a
K. Suga, *Japan*
H.J. Sung, *Korea*
J. Szmyd, *Poland*
A. Tomboulides, *Greece*
P. Tucker, *UK*
L. Vervisch, *France*
S. Wallin, *Sweden*
H. Yoshida, *Japan*
Z. Zhang, *China*

Patronage/Sponsors/Donators

Academy of Sciences and Arts of BH
Mayor of City of Sarajevo, *BH*
The University of Sarajevo, *BH*
International University of Sarajevo, *BH*
Delft University of Technology, *The Netherlands*
Sapienza University of Rome, *Italy*
Tokyo Institute of Technology, *Japan*
Electricité de France – R&D, *France*
AVL-List GmbH, *Austria*

Viessmann, *Croatia*
UNDP, *BH*
HVAC, *BH*
Mountain, *BH*
Interklima, *BH*
Weishaupt, *BH*
AluCo & Co.*BH*
Energy Design, *BH*
Bosna-S Eng., Oil&Gas, *BH*